# Modeling the Effects of Biological Tissue on RF Propagation from a Wrist-Worn Device

Jared D. Wilson-*EMBS Member*, Justin A. Blanco, Scott Mazar, Mark Bly

***Abstract – Many wireless devices in common use today are worn either on or in close proximity to the body. Among them are a growing number of wrist-mounted devices designed for applications such as activity or vital-signs monitoring, typically using Bluetooth technology to communicate with external devices. Here, we use a tissue-mimicking phantom material in conjunction with anechoic chamber and network analyzer testing to investigate how antenna propagation patterns in one such device are influenced by the electrical properties of the human wrist. A microstrip antenna module is mounted onto phantom material of various geometries, and the resulting voltage standing wave ratio (VSWR), input impedance, and azimuth radiation pattern are recorded in both free space and real-world environments. The results of this study demonstrate how the high permittivity values of human tissue ($\varepsilon_r \approx 16$) affect the design parameters of microstrip antennas. A simulation environment using Sonnet EM software was used to further analyze the high dielectric effects of biological tissue on RF propagation.***

## I. Introduction

This work addresses how the performance of a transmitting antenna mounted inside a wrist-worn wireless device may be influenced by the presence of the human wrist. We address this question by using a tissue-mimicking phantom material to simulate the electrical and geometric properties of the wrist. The interaction between electromagnetic waves and biological tissues is a widely studied area. Common research foci in this domain include the adverse health effects of electromagnetic waves on the human body [1]-[3]; the energy-absorption properties of biological tissue [4]-[8]; and the impact of biological tissue on the efficiency of wireless systems [9]-[12]. The present work falls into the latter category.

Previous studies have characterized the effect that biological tissue has on electromagnetic waves through a number of different methods including specific absorption rate [4]-[5], path loss models [6]-[8], and dielectric properties [9]-[12]. Studies of the specific absorption rate of biological tissue [4]-[5] produced results that elucidate the interaction between human tissue and electromagnetic waves. Kivekas et al. [5] specifically studied the interaction between the electromagnetic waves created by small antennas and nearby biological tissue. They concluded that the electrical properties of human tissue attenuate the perpendicular electric field components in a dipole antenna but did not study the influence of biological tissue on important antenna design parameters. Kurup et al. [6] used simulation and physical testing of a dipole antenna to create a path loss model within biological tissue. The path loss model confirmed that human tissue is a lossy medium that can be effectively modeled using 3D electromagnetic software (SEMCAD-X). The results from [6] would be useful in creating a link budget for a wireless system but are less applicable to the area of antenna design.

Dissanayake et al. [9] conclude that the varying permittivity values of human tissue affect the overall impedance matching characteristics of an implanted wireless system, resulting in poor efficiency and greater power demand. Studies on the use of an insulator with a dielectric constant that matches that of the human tissue [9], the use of substrates with high dielectric constants [13]-[14], and the use of a superstrate [15] have been conducted to partially correct the impedance mismatch in implantable wireless devices. While the aforementioned studies investigated the effects of biological tissue specifically on implantable antennas surrounded on all sides by biological tissue, the present work explores the effects that the wrist tissue has on the design parameters of an external, wrist-mounted wireless device. A network analyzer and an anechoic chamber were used to measure the effects of the phantom material on antenna performance. We used antenna gain, pattern, voltage standing wave ratio (VSWR), and input impedance to characterize performance.

## II. PHANTOM MATERIAL

### A. Creation

The skin-mimicking phantom material used here was described by Karacolak et al. [16]. It was designed for testing wearable devices in the industrial, scientific, and medical (ISM) band, which includes the frequency band of interest for this study (Bluetooth: 2.4-2.48 GHz). Karacolak et al. [16] show that their skin-mimicking gel accurately matches the conductivity ($\sigma$) and permittivity ($\varepsilon$) values of a biological tissue reference in the ISM band. The material is made from a sucrose (53%) and deionized water (47%) solution mixed with 1 gram of dry agarose per 100 mL [16]. More detailed instructions on formulating the material can be found in [16].

### B. Phantom Material Geometry

Two phantom material geometries were used in this study: a 4.5x4.5x1.19 in. box and an elliptic cylinder (diameters: 2.56x1.38 in.; length: 4 in.) designed to mimic the average

Research supported by the United States Naval Academy Bowman Scholar Program and by the DARPA Service Academies Innovation Challenge Program.

J. D. Wilson is with the United States Naval Academy, Annapolis, MD 21402 USA (phone: 740-438-9816; e-mail: jared.d.wilson24@gmail.com).

J. A. Blanco, is with is with the United States Naval Academy, Annapolis, MD 21402 USA (e-mail: blanco@usna.edu).

Scott Mazar is with Aclaris Medical, LLC, Saint Paul, MN 55114 (e-mail: smaz@iname.com).

Mark Bly is with Aclaris Medical, LLC, Saint Paul, MN 55114 (e-mail: mark.bly@aclarismedical.com).

male wrist. Both materials were made of acrylonitrile butadiene styrene (ABS) plastic. The wrist mold was built on a 3-D printer (Replicator 2, MakerBot Technologies, Brooklyn, NY). Each plastic mold was filled with the phantom material and provided shape as well as structural support to the phantom material. The box and wrist phantom structures are shown in Fig. 1 and Fig. 2, respectively.

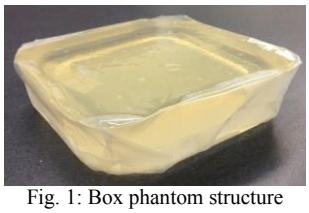

Fig. 1: Box phantom structure

Fig. 2: Wrist phantom structure

## III. REAL-WORLD TESTING

### A. Methodology

Real-world testing was conducted in an ordinary room that did not include any experimentally placed interfering sources. The VSWR and input impedance parameters of a microstrip dipole antenna were measured using a RF Vector Network Analyzer (N9923A FieldFox, Agilent Technologies, Santa Clara, CA) in this environment. A dipole microstrip antenna, shown in Fig. 3, was used for testing and was designed for use in the 2.3-2.5 GHz band [17]. FR-4 epoxy glass was used as the substrate ($\varepsilon_r \approx 4.5$).

VSWR and input impedance measurements were collected under four different conditions: 1) antenna only; 2) antenna with box structure in close proximity; 3) antenna with wrist structure in close proximity; and 4) antenna with human wrist in close proximity. The measurements were made using the configuration shown in Fig. 4, with each respective structure held in the elastic wrist band. Five measurements of the VSWR and input impedance were taken from 2.2-3 GHz for each experimental condition. The measurements were then averaged together and plotted using MATLAB (The Mathworks, Natick, MA).

Fig. 3: Microstrip dipole antenna used for testing with phantom material

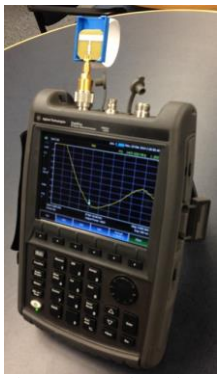

Fig. 4: Network analyzer configuration for initial testing

### B. Results

Plots comparing the VSWR and input impedance for each of the four conditions are shown in Fig. 5 and 6 respectively.

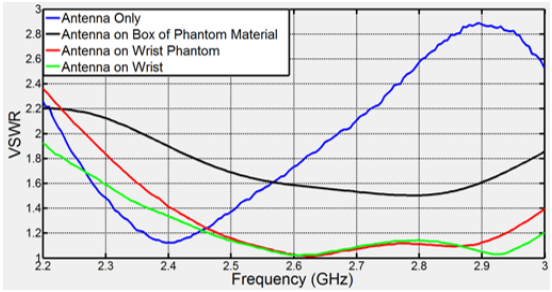


Fig. 5: RF Network analyzer measurements of VSWR for microstrip antenna

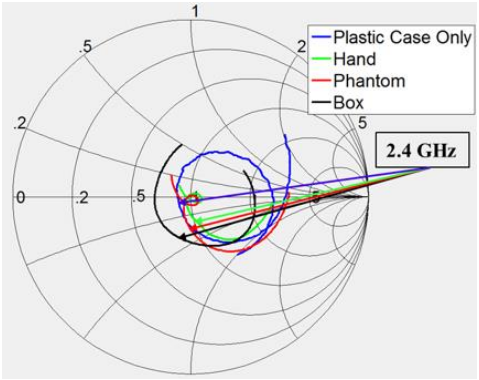


Fig. 6: RF network analyzer measurements of input impedance for microstrip antenna

The network analyzer measurements demonstrated the similarities in performance between the phantom material and the human wrist. Fig. 5 shows that the antenna's VSWR in the presence of a human wrist varies by a magnitude of less than 0.1 in the bandwidth of interest (2.4-2.5 GHz) when compared with the phantom wrist Greater variation can be seen at higher and lower frequencies, as the phantom material was specifically designed for the ISM band [16]. Fig. 6 shows the measured input impedance of the antenna. It can be seen that the dielectric properties of both the wrist and phantom material have a large effect on the input impedance of the antenna. The value for input impedance at 2.4 GHz is annotated in Fig. 6. While the real component of input impedance varied between the human wrist and phantom wrist, the imaginary components were almost identical, verifying that the phantom material and human wrist created similar capacitive effects on the antenna.

The geometry of the human tissue simulant also had a large impact on microstrip antenna performance. As shown in Figs. 5 and 6, there is a large deviation between the antenna in close proximity to the box and to the wrist, for both the VSWR and input impedance measurements.

## IV. ANECHOIC CHAMBER RESULTS

An anechoic chamber was used to approximate a free space environment. The microstrip dipole antenna used for real-world testing was mounted in the anechoic chamber, both isolated from and tangential to the phantom material wrist model, and an azimuth cut was recorded at 2.4035 GHz. The anechoic chamber and mounting configuration are shown in Figs. 7 and 8, respectively.

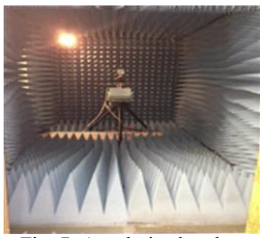

Fig. 7: Anechoic chamber

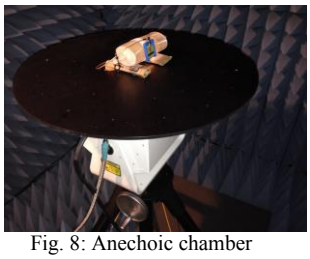

Fig. 8: Anechoic chamber mounting configuration

In the absence of the phantom material, the antenna's propagation pattern was nearly omnidirectional, as expected. The insertion of the wrist model into the anechoic chamber resulted in considerable attenuation and distortion of the propagation pattern, as seen in Fig. 9. As previously mentioned, the change in input impedance caused by the phantom material caused the decline in the overall performance of the antenna. Fig. 10 shows the input impedance of the microstrip antenna. Of note is that the real component of the impedance between 2.4-2.48 GHz remains relatively constant while the imaginary component changes due to the introduction of the high dielectric phantom. The phantom material increases the capacitive component of the input impedance of the antenna, causing the antenna's effective matching network to diverge from the ideal 50Ω. As a result, the amount of energy reflected back to the source increases, causing less energy to be emitted via the antenna.

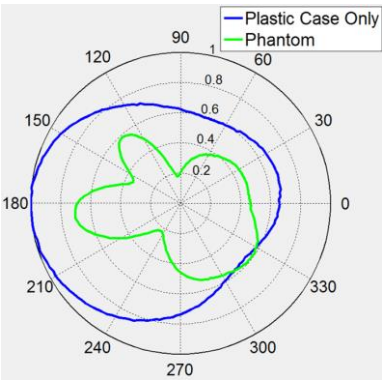


Fig. 9: Normalized anechoic chamber measurement for azimuth cut propagation pattern of dipole antenna at 2.403 GHz.

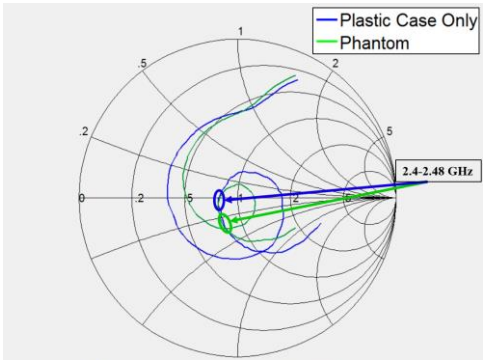


Fig. 10: Anechoic chamber measurements for input impedance of dipole antenna at 2.4305 GHz.

## V. Computer Simulation of Biological Tissue

### A. Concept

Sonnet Suites™, Electromagnetic Software [18], was used to model the effect of biological tissue on the design parameters of microstrip antennas. Sonnet utilizes dielectric layers in order to create a three-dimensional representation of the test environment for the microstrip circuit. Sonnet was used to model the high dielectric biological tissue ($\varepsilon \approx 16$). The complete three-dimensional view of the Sonnet test environment used can be seen in Fig. 11.


Fig. 11: Three-dimensional view of dielectric layers used in Sonnet antenna modeling

The antenna circuit was created in Sonnet by building the dipole antenna atop the biological tissue substrate. The input signal was placed in the center of two quarter-wavelength poles. A parameter sweep was conducted to find the optimal dipole length that minimized VSWR in the 2.4-2.48 GHz band. Two antennas resulted from this procedure: one for operation in free space (L = 28mm) and one for operation near biological tissue (L = 25mm). The lengths were confirmed using equation (1) (λ, wavelength; f, frequency; $\varepsilon_r$, relative permittivity). Equation (1) demonstrates why the high dielectric properties of biological tissue ($\varepsilon_r$ = 16) resulted in a shorter relative wavelength. The antenna model from Fig. 11 can be seen in more detail in Fig. 12.

$$\lambda = \frac{3.0 \times 10^8}{f \times \sqrt{\varepsilon_r}} \qquad (1)$$

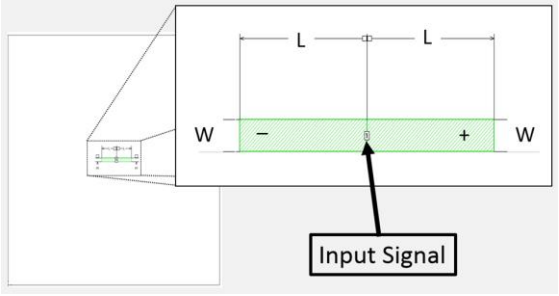


Fig. 12: Three-dimensional view of a proposed antenna design in Sonnet.

### A. Analysis Results

As expected, computer simulation demonstrated detuning effects of the phantom material similar in magnitude to those seen in physical modeling. Sonnet results for microstrip dipoles operating between 2 and 3 GHz are shown in Fig. 13.

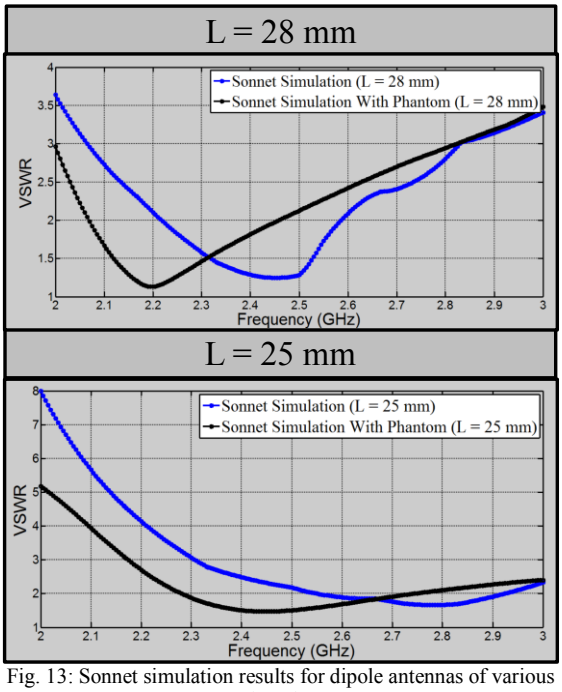

Fig. 13: Sonnet simulation results for dipole antennas of various lengths

A shift of approximately 300 MHz in the minimum VSWR is seen between the phantom and non-phantom conditions for both the 28mm and 25mm dipole lengths. The difference in antenna feeding methods is one possible explanation for the downshift in frequency observed in computer simulation as compared to the upshift seen in physical modeling. Future computer simulation of dipole antennas that utilize a matching network, as was used in physical simulation, can be used to confirm this hypothesis.

## VI. Conclusion

The goal of this study was to explore the effects that the electrical properties and geometry of the human wrist have on Bluetooth antennas in wrist-worn wireless devices. Better understanding these effects is integral to creating power-efficient wrist-worn wireless systems. Simulation results suggest that wrist tissue has an effect on the performance of wrist-worn antennas similar to that seen in prior studies using implantable antennas. Moreover, the effect that simulated human tissue has on the performance of wrist-worn antennas varies based on tissue geometry. Through Sonnet simulation, biological tissue was modeled to approximate the detuning affect caused by the high dielectric properties. This research provides a framework for future studies in antenna optimization for near-wrist performance.

## Acknowledgment

Dr. Anderson, Electrical Engineering professor at the United States Naval Academy, provided technical assistance in anechoic chamber testing.

## References

[1] Aggarwal, A., & Gupta, A. (2011). Effect of electromagnetic radiations on humans: A study. IEEE Technology Students Symposium, 75–80.

[2] Ubeid, M. F., & Shabat, M. M. (2010). Effect of negative index of refraction in the propagation of electromagnetic waves. Physics and Engineering of Microwaves Millimeter and Submillimeter Waves MSMW 2010 International Kharkov Symposium on.

[3] S. Gabriel, R. W. Lau, and C. Gabriel, "The dielectric properties of biological tissues: III. Parametric models for the dielectric spectrum of tissues" Phys. Med. Biol., vol. 41, pp. 2271–2293, 1996.

[4] R. A. Abd-alhameed, P. S. Excell, S. Member, and M. A. Mangoud, "Computation of Specific Absorption Rate in the Human Body due to Base-Station Antennas Using a Hybrid Formulation," vol. 47, no. 2, pp. 374–381, 2005.

[5] O. Kivekas, T. Lehtiniemi, and P. Vainikainen, "On the general energy-absorption mechanism in the human tissue," Microw. Opt. Technol. Lett., vol. 43, no. 3, pp. 195–201, Nov. 2004.

[6] D. Kurup, W. Joseph, G. Vermeeren, and L. Martens, "Path loss model for in-body communication in homogeneous human muscle tissue," Electron. Lett., vol. 45, no. 9, p. 453, 2009.

[7] S. K. S. Gupta, S. Lalwani, Y. E. E. Prakash, and L. Schwiebert, "Towards a propagation model for wireless biomedical applications," in IEEE Int. Commun. Conf., May 2003, vol. 3, pp. 1993–1997.

[8] L. C. Chirva, P. A. Hammond, S. Roy, and D. R. S. Cumming, "Radiation from ingested wireless devices in biomedical telemetry bands," Electron. Lett., vol. 39, no. 2, pp. 178–179, Jan. 2003.

[9] T. Dissanayake, K. P. Esselle, S. Member, and M. R. Yuce, "Dielectric Loaded Impedance Matching for Wideband Implanted Antennas," vol. 57, no. 10, pp. 2480–2487, 2009.

[10] N. Vidal and J. Sieiro, "Subcutaneous implanted antennas : interaction with biological tissues," 2008.

[11] W. Renhart, K. Hollaus, C. Magele, G. Matzenauer, and B. Weiss, "Radiation of USB-WLAN Antenna Influenced by Human Tissue and by Notebook Enclosure," IEEE Trans. Magn., vol. 43, no. 4, pp. 1345–1348, Apr. 2007.

[12] C. P. Hancock, S. Member, N. Dharmasiri, M. White, and A. M. Goodman, "The Design and Development of an Integrated MultiFunctional Microwave Antenna Structure for Biological Applications," vol. 61, no. 5, pp. 2230–2241, 2013.

[13] P. Soontornpipit, C. M. Eurse, and Y. C. Chung, "Design of implantable microstrip antenna for communication with medical implants," IEEE Trans. Microw. Theory Tech., vol. 52, no. 8, pp. 1944–1955, Aug. 2004.

[14] C.-M. Lee, T.-C. Yo, and C.-H. Luo, "Compact broadband stacked implantable antenna for biotelemetry with medical devices," in IEEE Annu. Wireless Microw. Technol. Conf., Dec. 4–5, 2006, pp. 1–4.

[15] R.Warty, M. Tofighi, R. U. Kawoos, and A. Rosen, "Characterization of implantable antennas for intracranial pressure monitoring: Reflection by and transmission through a scalp phantom," IEEE Trans. Microw. Theory Tech., vol. 56, no. 10, pp. 2366–2376, Oct. 2008.

[16] T. Karacolak, A. Z. Hood, and E. Topsakal, "Design of a Dual-Band Implantable Antenna and Development of Skin Mimicking Gels for Continuous Glucose Monitoring," IEEE Trans. Microw. Theory Tech., vol. 56, pp. 1001–1008, 2008.

[17] M. H. Jamaluddin, M. K. A. Rahim, M. Z. A. A. Aziz, and A. Asrokin, "Microstrip dipole antenna for WLAN application," 2005 1st Int. Conf. Comput. Commun. Signal Process. with Spec. Track Biomed. Eng., 2005.

[18] Sonnet Suites, www.sonnetsoftware.com.